

Performance of Multistatic Space-Time Adaptive Processing

Donald Bruyère

Department of Electrical and Computer Engineering, The University of Arizona
1230 E. Speedway Blvd., Tucson, AZ 85721
Phone: 520-349-3992, Fax: 520-626-3144
dbruyere@ece.arizona.edu

Nathan A. Goodman

Department of Electrical and Computer Engineering, The University of Arizona
1230 E. Speedway Blvd., Tucson, AZ 85721
Phone: 520-621-4462, Fax: 520-626-3144
goodman@ece.arizona.edu

Abstract - In this paper, we analyze the benefits of using multiple airborne radar systems viewing a scene from different directions. The filter outputs from multiple radars employing space-time adaptive processing (STAP) are combined to increase signal-to-interference-plus-noise ratio (SINR) and detection performance. The performance improvement is analyzed by looking at the detection probability and the probability of false alarm of the combined system with and without bistatic components of the multistatic system. Performance is compared to a multi-radar system employing a decentralized method of detection. Sensitivity to training data availability for adaptive filtering is also considered.

I. INTRODUCTION

Multistatic radars can provide improved performance against stealth targets, protection against attack through the use of standoff transmitters, and improved performance against electronic countermeasures. Due to these benefits, multistatic radar has been a popular area of research at several times in the last few decades. Currently, the deployment of unmanned air vehicles (UAV's) are again making multistatic radar systems and signal processing an interesting field of study.

The purpose of this paper is to analyze the benefits of using multiple airborne radar platforms to improve detection of moving targets in the presence of ground clutter. Historically, multi-sensor radar detection has been approached in two ways: centralized and decentralized. Decentralized methods makes detection decisions at each of the individual sensors, then fuse them together at some central point. One motive for the decentralized approach is the fact that communication bandwidth can be reduced since only binary detections need to be shared rather than

raw data [1-2]. Centralized multistatic radar systems are those that employ one or more radar sensors receiving signals from one or more transmitter platforms. These may employ both monostatic and bistatic configurations [3]. Whether bistatic and/or monostatic configurations are used, the multistatic system combines the signals into a single detection statistic, and detection is based on this value. Much of the work performed in this area involves ground-based transmitters and receivers where the clutter environment is non-moving and well defined [3-4].

This paper looks at multistatic space-time adaptive processing (STAP) deployed across multiple airborne platforms. We investigate the improvement in SINR and detection probability realized by noncoherently combining the space-time data from multiple airborne radar sensors. We also look at the behavior of multistatic STAP performance with respect to the amount of training data used for characterizing the clutter statistics.

Space-time processing exploits spatial and temporal signal properties to enhance radar detection in the presence of ground clutter [5]. But even with space-time processing, a target with a velocity vector perpendicular to the line of sight to the radar has the same Doppler shift as the surrounding background, making the target indistinguishable from clutter. However, a second radar looking at the same target from a different aspect angle may observe enough Doppler shift to distinguish the target from ground clutter. By applying this concept to radars that employ space-time processing, large improvements can be realized in the combined system's signal-to-interference-plus-noise ratio (SINR), thus improving target detectability. We call this the geometry gain of multistatic STAP (see Figure 1). Related to this advantage is the potential of the multistatic system to estimate absolute velocity, not just radial velocity.

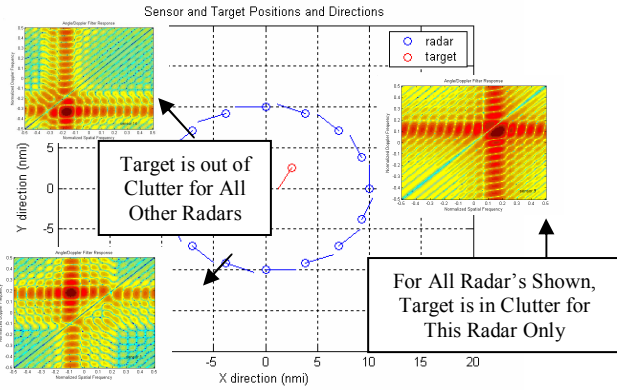


Figure 1. Geometry Gain - Moving targets that are buried in clutter for one radar aspect angle are likely to be out of clutter for a radar at another aspect

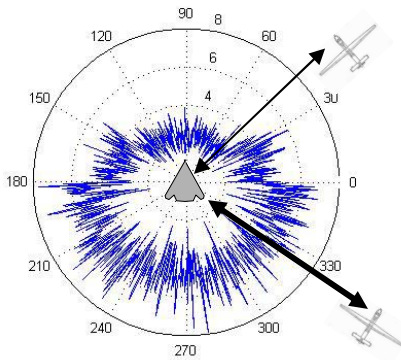


Figure 2. Diversity Gain - Targets that have faded for one radar may have a strong return for another radar

Since target returns have a tendency to fluctuate from one measurement to the next, viewing a target return from multiple locations gives more opportunities to view the target when it's return is strong for at least one of the viewing radars, even though it's return has faded for other radars (see Figure 2) [6]. The advantage associated with this aspect of multiple viewing perspectives is referred to as a diversity gain.

In this paper, we look at the performance gains in detection probability realized by combining the data from several airborne radar platforms performing space-time adaptive processing. We present the combining rule used to produce the aggregate test statistic associated with a system of multiple airborne radars viewing a scene from distributed locations. Then we compare the performance of joint detection with that of a decentralized detection approach, each using multiple platforms possessing coherent space-time radars. As a matter of practical concern, we also investigate the effects of limited training data on both the optimum and decentralized approaches.

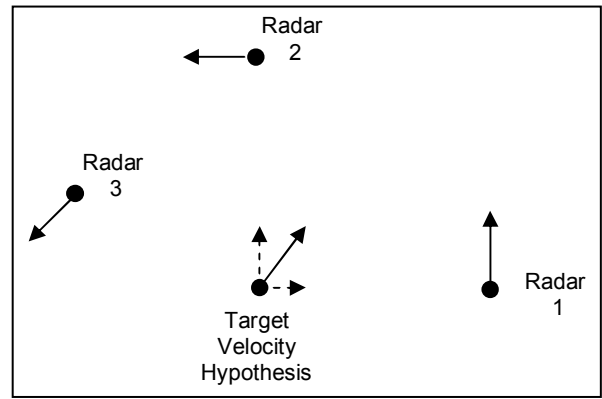


Figure 3. Radar/target geometry for multistatic STAP study.

II. SIGNAL MODEL AND DETECTION STATISTIC

Figure 3 illustrates a potential multistatic geometry. A set of airborne platforms is overlooking the same field of view. Each platform is equipped with a multi-channel coherent radar. For any single radar platform, a target that is not moving radially toward or away from that radar would be indistinguishable from background clutter.

Let the multistatic radar system be defined by K independent sets of space-time observations of the geographical area. The data sets may consist of both monostatic and bistatic collection geometries. The independence from space-time data set to space-time data set is due to the geographical separation of the radar platforms. Let the k^{th} space-time data set be denoted by the vector \mathbf{y}_k for $1 \leq k \leq K$. The space-time data samples associated with a single monostatic or bistatic collection are *stacked* into a length- $N_k M_k$ column vector where $N_k M_k$ is the number of space-time measurements in the k^{th} data set. This will be referred to as a single radar space-time snapshot with $N_k M_k$ degrees of freedom.

Every data vector comes from one of two potential hypotheses:

$$\left. \begin{aligned} H_0 : & \quad \mathbf{y}_k = \mathbf{n}_k \\ H_1 : & \quad \mathbf{y}_k = a_k \exp(j\phi_k) \mathbf{s}_k + \mathbf{n}_k \end{aligned} \right\} \quad (1)$$

where H_1 denotes the target-present hypothesis and H_0 indicates the target-absent hypothesis. Every snapshot contains the noise vector, \mathbf{n}_k , which is composed of a spatially and temporally white Gaussian thermal component, as well as a colored Gaussian clutter component. Note that the correlated interference due to clutter is only correlated between measurements collected by the same platform for the same geometry, while the interference is assumed to be independent from data set to data set due to being collected on distinct

platforms and/or geometries. The noise vector for the k^{th} data set is characterized by the covariance matrix \mathbf{R}_k . The H_1 hypothesis has a fluctuating target signal with Rayleigh distributed amplitude, a_k , and uniformly distributed phase, ϕ_k . The target's space-time steering vector relative to the k^{th} data set is \mathbf{s}_k .

We assume that each radar can be configured to receive its own return as well as the other radars' returns in a bistatic configuration. This could be accomplished, for example, by causing each transmitter to operate in different frequency bands that could be separately filtered and sampled by each radar receiver. Due to the geometric separation of the platforms, target reflection coefficients are modeled as independent from platform to platform but constant over the local data collected by a single platform. Likewise, clutter statistics are assumed independent from platform to platform but have a local space-time correlation structure typical of airborne space-time adaptive processing. Given these assumptions, the log-likelihood ratio test (LRT) for multistatic detection of the Rayleigh-fluctuating target is

$$\overline{\ln \Lambda(\mathbf{y})} = \sum_{k=1}^K \frac{r_k^2}{\frac{1}{A_k^2} + 2\mathbf{s}_k^H \mathbf{R}_k^{-1} \mathbf{s}_k} = \zeta \quad (2)$$

where A_k is the Rayleigh parameter that controls the average RCS of the target for the k^{th} data set and where

$$r_k = \left| \mathbf{w}_k^H \mathbf{y}_k \right| \quad (3)$$

represents the output of the locally optimum STAP filter, $\mathbf{w}_k = \mathbf{R}_k^{-1} \mathbf{s}_k$, applied to the k^{th} data vector, \mathbf{y}_k . In (2), it is seen that the usual single-platform STAP output is scaled by a factor that is a function of two components: 1) the amount of interference having similar space-time spectral characteristics as the target, 2) the Rayleigh parameter, which is related to the target's average RCS. If the target's power is small when compared to the background interference for a given platform, then the contribution from that platform is de-emphasized before combining with the other platforms making up the multistatic system. On the other hand, if the average RCS of the target is large compared to the background noise environment, then that platform's output is weighted more heavily in the overall test statistic.

In a single-platform STAP scenario, the filter output can be neatly separated into signal and interference components, which leads to a situation where the ratio of output signal power to average

output noise power can be computed. In the multistatic case described by (2), however, the contributions from individual data sets are squared prior to being combined in the final detection statistic. This causes signal/noise cross terms to appear in the total detection statistic under the target hypothesis, making the standard definition of output SINR difficult to apply because signal and noise cannot be cleanly separated. Therefore, in this paper we apply an alternative definition of SINR. This definition, also used in [6] and called the deflection coefficient in [7], quantifies the separation in the test statistic associated with the H_1 and H_0 hypotheses, and thereby, gives a metric of SINR that we can use to analyze the relative gain realized by combining the outputs of several radars into one system. Given the pdf's of the two hypotheses, we define

$$SINR = \frac{|E[\zeta/H_1] - E[\zeta/H_0]|^2}{\frac{1}{2}(Var[\zeta/H_1] + Var[\zeta/H_0])} \quad (4)$$

where $E[\zeta/H_i]$ is the expected value of the test statistic under hypothesis i , and $Var[\zeta/H_i]$ is the variance of the test statistic, under hypothesis i . Although the deflection coefficient strictly indicates performance only in the case where the detection statistic is Gaussian-distributed under both hypotheses, we have observed that this SINR metric is useful for approximating the geometry and diversity benefits associated with multistatic STAP.

III. PERFORMANCE RESULTS

Figure 4 demonstrates the geometry gain realized by a multistatic system. This is demonstrated by plotting the SINR performance, as defined by (4), versus two target velocity components for a three-radar configuration. From the figures, three basic regions can be identified. In the first region, the target is moving slowly or not at all; therefore, it falls into the clutter ridge no matter what geometry is applied or how many platforms observe it. This results in a deep notch in performance around an absolute velocity of zero. In the second region, the target is moving nearly perpendicular to one of the radars; hence, it falls into the clutter ridge for one radar but not the others. SINR performance from this region is greatly improved over the first region. SINR performance is best, however, in the third region where the target's velocity vector has significant components toward multiple radars. In this case the target is out of the clutter ridge for all radars, and SINR performance is improved over the second

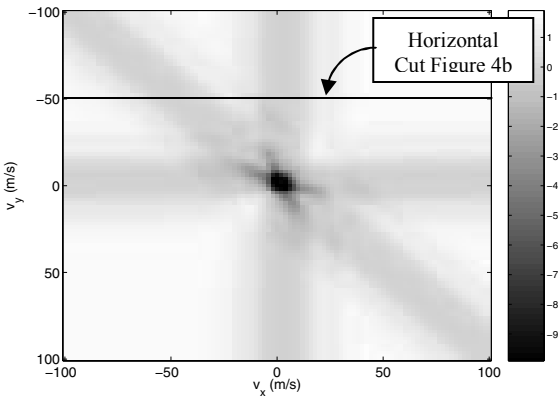


Figure 4a. Combined radar 1,2 & 3 SINR surface for target in Figure 3 for various velocity hypotheses.

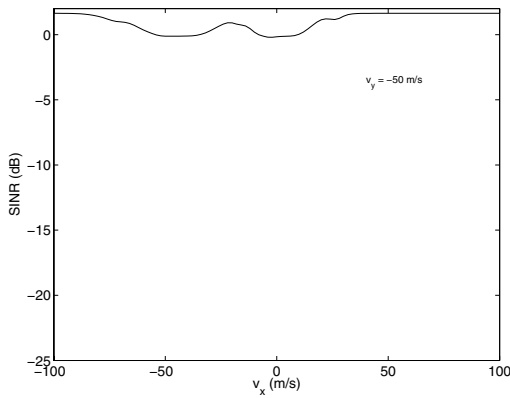


Figure 4b. SINR plot for target $V_y = -50$ m/s for various target V_x hypotheses (horizontal cut of Figure 4a).

region due to having three independent observations of a fluctuating target.

One reason for the performance gain is that the Doppler shift relative to each radar is different, so we realize a gain by virtue of the fact that a target that may be buried in clutter for one radar is not necessarily in clutter for other radars, provided they are not colocated. Moreover, even if a target falls outside the clutter ridge for multiple radars, there is still an additional diversity gain [6] that improves performance by virtue of multiple observations of a fluctuating/fading target [8].

Next, we look specifically at the detection improvement obtained by adding platforms. In this case, the multistatic configuration can consist of the monostatic data collected by each radar as well as the results from bistatic configurations between the radars. We only consider a single direction for each bistatic path. Therefore, for a two-radar configuration, only one bistatic path is exploited. With a three-radar configuration, three bistatic paths are exploited.

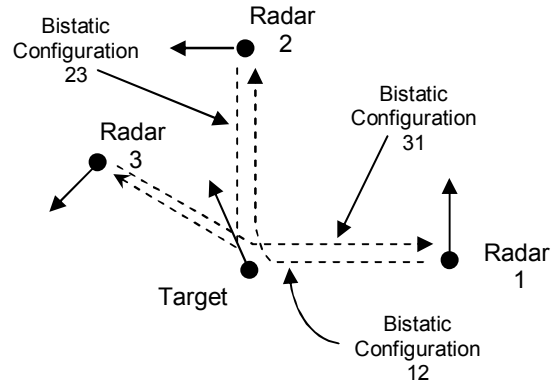


Figure 5. Multistatic configuration used for simulation of three-platform systems.

Figure 5 illustrates the bistatic geometry configurations¹ for a sample three-platform system.

Figure 6 compares the performance of multistatic STAP with that of a decentralized method of detection when only monostatic configurations are used in the detection statistic. The decentralized approach chosen was to allow each radar to produce its own binary decision, called the local decision. Then, the binary decisions are shared with a centralized processor, which makes a final decision based on a Boolean ‘OR’ operation².

In addition to studying the geometry and diversity gains provided by multistatic STAP, we are also interested in the relative performance between optimum and decentralized detection when the interference covariance matrix must be estimated from training data. In Figures 6 and 7, the sample covariance matrix was calculated as

$$\hat{\mathbf{R}}_k = \frac{\mathbf{Y}_k \mathbf{Y}_k^H}{L_k} \quad (5)$$

where \mathbf{Y}_k is the $N_k M_k$ -by- L_k matrix of independent, identically distributed realizations of interference for the k^{th} data set. This was used to calculate the local STAP filter weights as $\mathbf{w}_k^H = \hat{\mathbf{R}}_k^{-1} \mathbf{s}_k$. Although in practice, each platform will observe interference with different statistical properties, any choice for the different \mathbf{R}_k 's for the observing platforms in our simulation is arbitrary. Therefore, for simplicity, the same ideal clutter covariance characteristics were used for all radar platforms.

¹ For the purposes of this study, the resolution issues associated with bistatic geometries where the bistatic angles of greater than 90° are ignored [9] [10].

² The ‘OR’ rule was selected for comparison based on its superior performance over other fusion rules compared in reference [11].

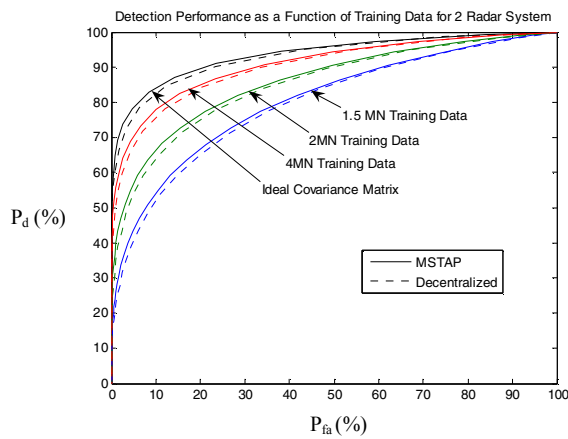


Figure 6a. Detection performance as a function of training data for a two-radar multistatic system.

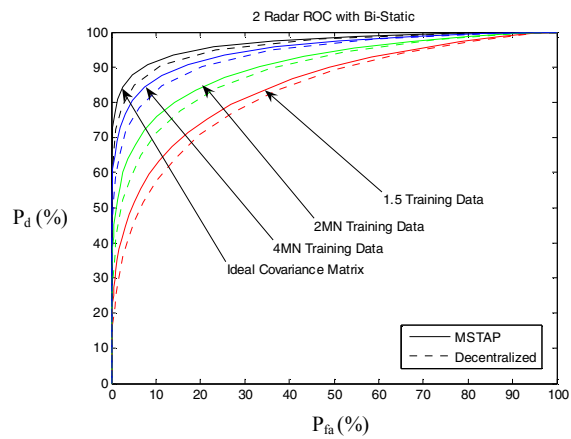


Figure 7a. Detection performance as a function of training data for a two-radar multistatic system with bistatic and monostatic data.

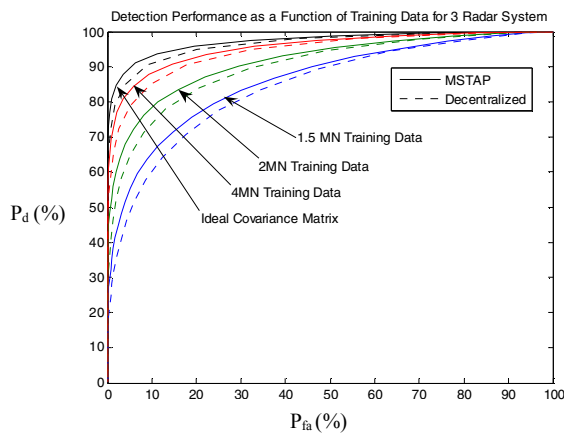


Figure 6b. Detection performance as a function of training data for a three-radar multistatic system.

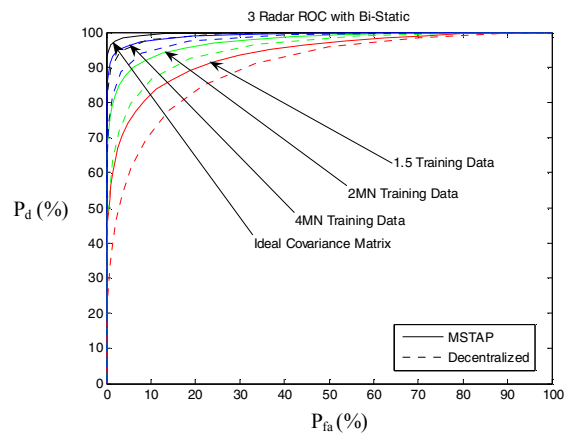


Figure 7b. Detection performance as a function of training data for a three-radar multistatic system with bistatic and monostatic data.

Three different training data sample sizes were run for both a two-radar and a three-radar geometry, and the detection results were compared to the detection performance of a system using an ideal covariance matrix. As a rule of thumb, monostatic STAP performance from a clutter covariance matrix estimated using $2NM$ snapshots will be about 3 db below ideal performance, where N is the number of array elements, and M is the number of pulses. Therefore, the three test cases chosen were for 1.5, 2, and 4 times the degrees of freedom of the system. For each case, Monte Carlo simulation was employed to generate test statistic output under both the target-present and target-absent hypotheses. From these test statistic outputs, the probability of detection and the probability of false alarm for varying detection threshold were computed. The resulting performance curves are shown in Figures 6 and 7. In Figure 6, only the monostatic data are used, while in Figure 7, the bistatic data have been added.

The analysis shows that adding radar platforms in a multistatic STAP configuration provides superior detection performance over both individual radars performing STAP as well as multiple radar configurations using a decentralized method of detection. For a multistatic STAP system using only monostatic data from a few platforms, the margin of improvement between multistatic and decentralized is not very large. In Figure 6, however, the margin seems to increase as the number of platforms increases. This effect can be seen in Figure 7 where the bistatic data are included. Since we have ignored resolution and training issues unique to bistatic radar, the bistatic data are, statistically speaking, very similar to the monostatic data. In Figure 7b, we are essentially combining six unique data sets, and it is seen that the performance margin between optimum and decentralized detection increases dramatically. When only monostatic data is employed in the multistatic system, the number of independent looks

increases linearly with the number of observing platforms. However, when the bistatic components are included in the combined system, the number of independent looks increases much more quickly. For the purposes of this analysis, only one independent look is included between any pair of radar platforms within the multistatic scenario. The reverse path of any given radar pair is not considered independent from the forward path since the target RCS fluctuation should be similar for any one given bistatic angle. Given this assumption, the number of total independent looks from combined monostatic and bistatic configurations in any multistatic geometry is $N_{radars}[(N_{radars}+1)/2]$.

Including the one-way bistatic components produces a dramatic difference in system performance of the centralized multistatic STAP system over the decentralized approach when the number of platforms employed is three or more. Hence, we conclude that although decentralized detection performs nearly as well as centralized multistatic STAP for a few radar platforms, the use of bistatic data may quickly provide a situation where centralized detection has significant benefit.

V. CONCLUSIONS

The purpose of this paper was to investigate the improvement in detection performance by noncoherently combining the space-time data from multiple airborne radar sensors. Performance was measured in two ways: 1) Using an SINR metric that measures the statistical separation between the probability distribution functions of the test statistic with and without the target present, 2) plotting probability of detection as a function of probability of false alarm for various receiver threshold settings. We also looked at that same performance as a function of SMI training data. This analysis was performed for a Multistatic STAP where only monostatic configurations were employed, then repeated with the one way bistatic components added.

When only monostatic was employed in the multistatic system, the number of independent looks increases linearly with the number of observing platforms. However, when the bistatic components are included, the number of independent looks received increases loosely as the square of the number of platforms employed. When the number of platforms in a combined mono/bistatic configuration is three or more a very dramatic increase in system performance is realized when compared to a decentralized approach. In either the monostatic or mono/bistatic cases, the margin of performance of the centralized Multistatic STAP approach over that of a

decentralized method was unaffected by the amount of training data employed.

In summary, while a decentralized detection method performs nearly as well as centralized multistatic STAP for a few radar platforms, the use of bistatic data may quickly provide a situation where centralized detection has significant benefit.

VI. REFERENCES

- [1] Li, T, Sethi, I.K., "Optimal multiple level decision fusion with distributed sensors", *IEEE Trans. on Aerospace and Electronics Systems*, vol. 29, no. 4, pp. 1252-1258, Oct. 1993.
- [2] Tenney, R.R., Sandell, N.R., "Detection with distributed sensors", *IEEE Trans. on Aerospace and Electronics Systems*, vol. AES-17, no.4, pp-501-509, July 1981.
- [3] Hanle, E., "Survey of bistatic and multistatic radar", *IEE Proceedings*, vol 133, pt. F, no.7, Dec. 1986.
- [4] Addio, E., Farina, A. "Overview of detection theory in multistatic radar," *IEE Proceedings*, vol 133, pt. F, no.7, Dec. 1986.
- [5] Melvin, W. L. "A STAP overview", *IEEE A&E Systems Magazine*, vol. 19, no.1, pp. 19-35, Jan. 2004.
- [6] Fisher, E, Haimovich, A., Blum, R., Cimini, L., Chizhik, D., Valenzuela, R. "Spatial diversity in radars – models and detection performance," to appear in *IEEE Trans. on Signal Processing*.
- [7] Steven M. Kay, *Fundamentals of Statistical Signal Processing, Vol. II: Detection Theory*. New Jersey: Prentice-Hall, 1998.
- [8] E. Conte, E. D'Addio, A. Farina, and M. Longo, "Multistatic radar detection: synthesis and comparison of optimum and suboptimum receivers", *IEE Proceedings*, vol. 130, part F, no. 6, pp. 484-494, Oct. 1983.
- [9] Hanle, E., "Survey of bistatic and multistatic radar," *IEE Proceedings*, vol. 133, part F, no. 7, pp. 587-595, Dec. 1986
- [10] Jackson, M.C., "The geometry of bistatic radar systems", *IEE Proceedings*, vol. 133, part F, no. 7, pp. 604-612, Dec. 1986
- [11] Srinivasan, R., Sharma, P., Malik, V., "Distributed detection of swerling targets," *IEE Proceedings*, vol. 133, part F, no. 7, pp. 624-629, Oct. 1986.